# Determination of the Plasma Delay Time in PIPS detectors for fission fragments at the LOHENGRIN spectrometer

*Ana M.* Gómez[1,*], *Ali* Al-Adili[1,**], *Alf* Göök[1], *Stephan* Pomp[1], *André* Pousette[1], *Andreas* Solders[1], *Diego* Tarrío[1], *Zhihao* Gao[1], *Ulli* Köster[3], *Yung Hee* Kim[3], *A. Gavin* Smith[5], *Nikolay V.* Sosnin[4], *Samuel* Bennett[5], *Tobias* Wright[5], *Andreas* Oberstedt[6], and *Stephan* Oberstedt[2]

[1]Department of Physics and Astronomy, Uppsala University, Box 516, 751 20 Uppsala, Sweden.
[2]European Commission, Joint Research Centre (JRC), 2440 Geel, Belgium.
[3]Institut Laue-Langevin, 38042 Grenoble, France.
[4]University of Edinburgh, EH9 3FD Edinburgh, United Kingdom.
[5]University of Manchester, M13 9PL Manchester, United Kingdom.
[6]Extreme Light Infrastructure - Nuclear Physics (ELI-NP), Horia Hulubei National Institute for Physics and Nuclear Engineering (IFIN-HH), 077125 Bucharest-Magurele, Romania.

**Abstract.**

The VElocity foR Direct particle Identification spectrometer (VERDI) is a 2E-2v fission spectrometer that allows the measurement of the total mass distribution of secondary fission fragments with a resolving power of 1-2 u. It consists of two time-of-flight (ToF) arms, with one Micro Channel Plate (MCP) detector and up to 32 Silicon PIPS (Passive Implanted Planar Silicon) detectors per arm. The MCPs provide the start timing signals and the PIPS detectors provide both the energy and the stopping ToF signals. In real conditions, the PIPS signals are affected by the formation of plasma from the interaction between the heavy ions and the detector material. The plasma contributes to a reduction in signal amplitude, resulting in a Pulse Height Defect (PHD), and introduces a signal delay, known as Plasma Delay Time (PDT). An experiment to characterize the PDT and PHD was performed at the LOHENGRIN recoil separator of the Institut Laue Langevin (ILL). Characteristic fission fragments from the $^{239}$Pu(n,f) reaction were separated based on their A/Q and E/Q ratios, allowing the measurement of a wide range of energies from 21 to 110 MeV and masses between 80 and 149 u. Six PIPS detectors were characterized to study their individual responses to the PDT and PHD effects. The signals were recorded in a digital acquisition system to completely exploit the offline analysis capabilities. Achieved combined timing and energy resolutions for fission fragments varied between 72(2) ps and 100(4) ps and 1.4% - 2% (FWHM), respectively. Preliminary PHD and PDT data are presented from the masses A=85, 95, 130 and 143. The PHD trends are strongly correlated with both the ion energy and mass. The PDT, on the other hand, shows a strong variation as a function of the ion kinetic energy but a smaller dependence on the ion mass.

## 1 Introduction

The particle spectrometer VERDI (VElocity foR Direct particle Identification) allows measurements of the pre- and post-neutron emission of the fission-fragment mass distributions. The goal of the VERDI-project is to achieve a mass resolution between 1 and 2 u [1, 2]. VERDI consists of two arms, each with up to 32 Passive Implanted Planar Silicon (PIPS) [3] detectors and a Micro Channel plate (MCP). The MCPs provide the pick-off signal used as the start of the time-of-flight (ToF) measurement, and the PIPS detectors are used for both measuring the energy and providing a stop signal for the ToF of the (secondary) fission fragments (FF). The measurement technique is based on the so-called double-energy double-velocity (2E-2v) method and can provide data on the fragment-specific average neutron emission. This method can complement other fission-neutron detection methods [4] to independently probe the excitation-energy sharing in nuclear fission.

In PIPS detectors, the interaction between heavy ions and the detector material is known to produce a dense cloud of charges (plasma). The plasma momentarily disturbs the electric field and, as a consequence, only charge carriers in the outer edge of the cloud will begin migration, leaving the inner charges temporarily stationary. The free electrons may, therefore, recombine with positive charge carriers, causing a smaller signal height. This effect is known as Pulse Height Defect (PHD) [5]. In addition, the plasma slows down the transit of the charge carriers producing a delay on the signals, which is know as the Plasma Delay Time (PDT) [5]. The PDT, with typical values between 2 ns and 5 ns for FF, leads to a wrong calculation of the FF mass-distributions and, therefore, to a wrong cor-

*e-mail: ana.gomez@physics.uu.se
**e-mail: ali.al-adili@physics.uu.se

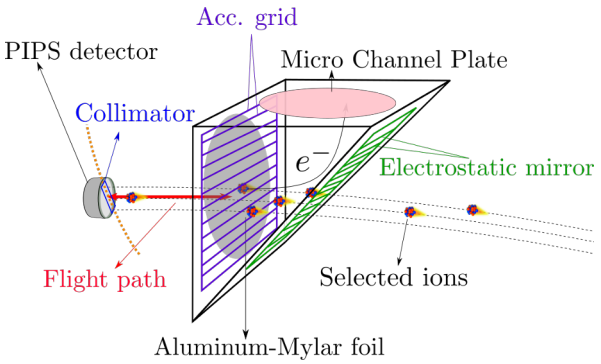


**Figure 1.** Schematic view of the experimental setup. A Micro Channel Plate Detector (MCP) provides a start time-of-flight signal by detecting electrons ejected from a Mylar foil. The stop time-of-flight and energy detection are made by the VERDI PIPS detector placed in front of the foil.

relation with other fission observables, as well as, an increase in systematic uncertainties [6, 7]. Earlier studies proposed different parametrisations to estimate the PDT and PHD contributions [8–11]. The literature functional dependencies of PDT($E, A$) and PHD($E, A$) indicate that different detector types seem to exhibit unique behaviours. Moreover, previous attempts to exploit the parameterisation from Ref. [8] on VERDI velocity data produced non-physical correlations between the average number of emitted neutrons and the Total Kinetic Energy (TKE). This motivated a dedicated experiment to study the PDT and the PHD in the type of detectors used in VERDI.

The LOHENGRIN recoil separator at the Institut Laue-Langevin (ILL), is perfectly suited for these investigations. Fission fragments with separated masses and energies can be selected to unambiguously determine the Pulse Height Defect and Plasma Delay Time. In this work, we discuss the experiment technique and data analysis methods as well as present preliminary results from masses $A$=85, 95, 130 and 143.

## 2 Experiment

The determination of the PDT and the PHD relies on the precise mass and energy knowledge from LOHENGRIN. By using a dedicated ToF section, one can determine the ion velocities and energies with the PIPS detectors and compared them with the settings of the LOHENGRIN spectrometer, to estimate the PHD and PDT, respectively.

### 2.1 Ion beam production

The LOHENGRIN recoil mass separator is a spectrometer connected to a beam tube of the high-flux reactor of the Institut Laue-Langevin (ILL). LOHENGRIN can produce high fluxes of separated ions with very high resolution. The spectrometer consists of two main sections: a dipole magnet and an electrostatic deflector. The dipole magnet filters ions based on their momentum-to-ionic charge ratio whereas the electrostatic deflector separates the ions based on their kinetic-energy to ionic-charge ratio E/Q. The combined action of both fields acts as Thomson parabola spectrometer where the focal plane forms a parabola representing ions separated according to a given mass-over-ionic charge ratio A/Q. The ions are separated according to their velocity along the parabola and, due to the fixed A/Q ratio by the parabola, according to their kinetic energy E.

The ion beam were produced using the $^{239}$Pu(n,f) reaction. A highly enriched $^{239}$Pu sample was placed close to the reactor core, where it was exposed to a thermal neutron flux of about $5{\times}10^{14}$ n s$^{-1}$ cm$^{-2}$ [13]. The target was deposited on a thick Ti backing and covered by a 0.25 $\mu$m thin Ni foil [14]. At the time of the experiment, the sample was relatively old and, therefore, the Pu had diffused into the backing. This causes additional ion energy loss to the FFs that are not formed at the surface of the target, making lower kinetic energies accessible. This feature made it possible to extend the PDT and PHD kinetic energy trends beyond typical fission-fragment ranges.

### 2.2 Setup

A schematic view of the experimental setup is shown in Fig. 1. The timing measurement starts in the ToF section, which is part of the Fission Fragment Identification setup (FiFI), developed as part of the STEFF fission spectrometer of the University of Manchester [15]. The ToF section has an isosceles right triangle shape, formed by a foil, an electrostatic mirror and a MCP. The double layer foil facing the ion beam has one layer of aluminum (thickness 256 Å) and another layer of Mylar (~1000 Å thickness), both deposited on top of a 1x1 cm$^2$ circular grid with 8 cm diameter made of steel wires (0.2 mm diameter). The ion passage through the foil leads to secondary electron emission, of which some are emitted backwards and accelerated by an initial grid, mounted a few millimeters in front of the foil. A second grid of wires with a diameter of 20 $\mu$m (electrostatic mirror), placed 45 degrees from the foil normal plane, deflects the electron cascade towards a Hamamatsu F1942-04 MCP, mounted in the upper part of the ToF section, and operated at 2.2 kV and a pressure lower than $10^{-7}$ mbar. The MCP multiplies the electron cascade to form the ToF-start signal.

The PIPS detectors were mounted on a movable arm which could be manipulated externally, in order to change the flight path without breaking the vacuum. Six Canberra PIPS detectors of type TMDP 450 -20N TD - 300 AM, operated with a bias voltage of 140 V, were mounted in two different holders. One holder hosts a single detector while the other hosts four detectors in a clover configuration, two of which can be irradiated simultaneously. The single holder kept the PIPS detector concentrically with respect to axis of the manipulator, which coincided with the central position of the focal plane. The position of each detector in the clover configuration was 23.5 mm off-center with respect to the focal plane. Each detector was collimated with a 5 mm wide slit, to prevent parasitic nearby masses from entering the PIPS detector.

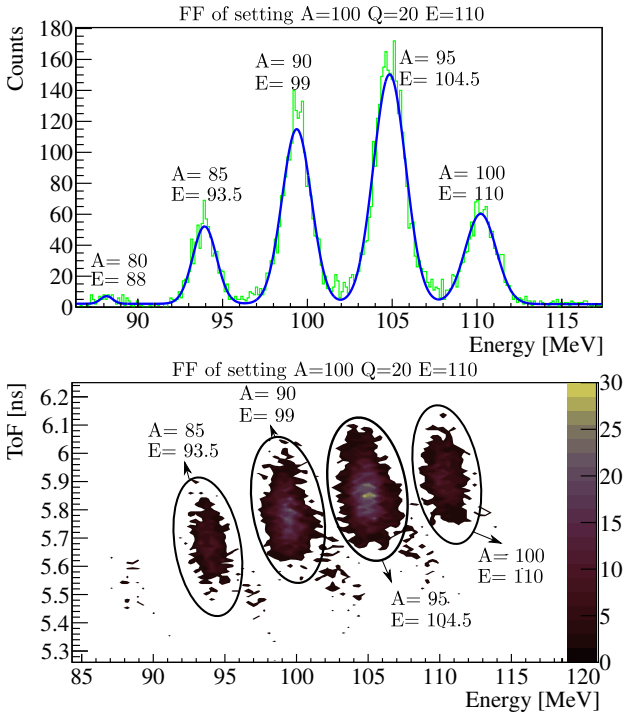


**Figure 2.** Top: Energy spectrum for the setting A=100, Q = 20 and E = 110 MeV. Bottom: time-of-flight as a function of the energy of data for setting A=100, E=110 and Q=20. The observed shift in the ToF is caused by the PDT.

### 2.3 Electronics and DAQ

The PIPS detectors were connected to MPR-1 Mesytec charge-sensitive pre-amplifiers. The modules were operated in a sensitivity suitable for FF spectroscopy. The F1942-04 MCP has an integrated pre-amplification and its signals were connected to a digitizer.

The pre-amplified signals were digitized with an ADQ412 SP Devices card and sent to a computer for an offline event-by-event analysis. The acquisition card has four channels, a sampling frequency of 1 GHz and 12-bits resolution. When a FF triggered a signal on the PIPS channel, the corresponding MCP signal was recorded.

### 2.4 Measurements

Measurements with six different PIPS detectors from VERDI were taken at LOHENGRIN. A total of 24 magnet settings for heavy ions were used, 7 settings for $\alpha$-particles, three more for protons and finally one setting for triton. The various measurements were taken at similar but well-calibrated flight path distances from the MCP foil, typically around 4 cm. The resulting masses for each setting cover a range from 80 u to 149 u with energies between 21 MeV to 110 MeV. The light particles were measured in order to ultimately estimate the PDT and PHD values of FFs, $\alpha$-particles and tritons relative to the protons.

A typical spectrometer setting is shown in Fig. 2. Only those fragments with A/Q and E/Q ratios equal to the chosen settings will reach the PIPS detector. The intensity of each peak in the resulting distribution is governed by the $^{239}$Pu(n,f) mass, kinetic energy and charge state yield .

## 3 Analysis

### 3.1 Digital signal processing

The timing information was deduced from the digital waveforms, after applying a CR(RC) (Capacitor-Resistor Resistor-Capacitor) filter, followed by a Constant Fraction Discriminator (CFD) to both PIPS and MCP signals, with dedicated optimized parameters. To determine the ion energy, a CR(RC)$^4$ filter was applied [16].

A careful fine-tuning of parameters during digital signal processing resulted in a combined ToF resolution between 72(2) ps and 100(4) ps and 1.4% - 2% in energy peak resolution (FWHM) for FF.

### 3.2 Time-of-flight and energy calibration

Alpha particles, protons and tritons were all measured at different energies, and serve for both energy and ToF calibrations. For FFs, the energy and time calibrations are performed relative to $\alpha$-particles, i.e. we assume that $\alpha$-particles do not suffer from PHD or PDT effects. The calibration relative to $\alpha$-particles is most relevant for VERDI, since $\alpha$-particle sources are generally available for calibration. Thereby, the results of the present experiment can be directly applied in future experiments with VERDI. However, for the sake of a complete systematic characterisation, the PDT and PHD of $\alpha$-particles will eventually be calculated relative to protons and tritons, using a dedicated measurement performed with a higher pre-amplifier sensitivity.

A linear energy calibration of the Si detectors was performed using the 4.75 MeV and 12 MeV $\alpha$-particles, after correcting for their energy losses. The energy losses of the ions, in the aluminum-mylar foil and the Si dead layer, were calculated using a Geant-4 model described in Ref. [17]. The ToF offset was determined as the difference between the calculated ToF of the 4.75 MeV $\alpha$-particle and the mean value of its measured ToF distribution, as obtained from a Gaussian fit.

### 3.3 Particle identification of detected ions

As mentioned earlier, each setting leads to a set of masses and energies that satisfy the A/Q and E/Q ratio selections in LOHENGRIN. In order to identify the observed ion peaks, one setting has to serve as a calibration case. For this initial identification, a reference setting was chosen (A=100, E=110 MeV), where the ionic charge was set once to Q=20 and once to Q=22. In both settings A=100 will appear at the same position in the spectrum (corresponding to E=110 MeV) while other masses with similar A/Q but different E will shift. This operation implies that ions with mass number 100 and at 110 MeV appear at the same peak position in the Silicon detector, at the same time new mass peaks appear in the spectrum at different pulse heights. This particle identification is then extrapolated to other settings.

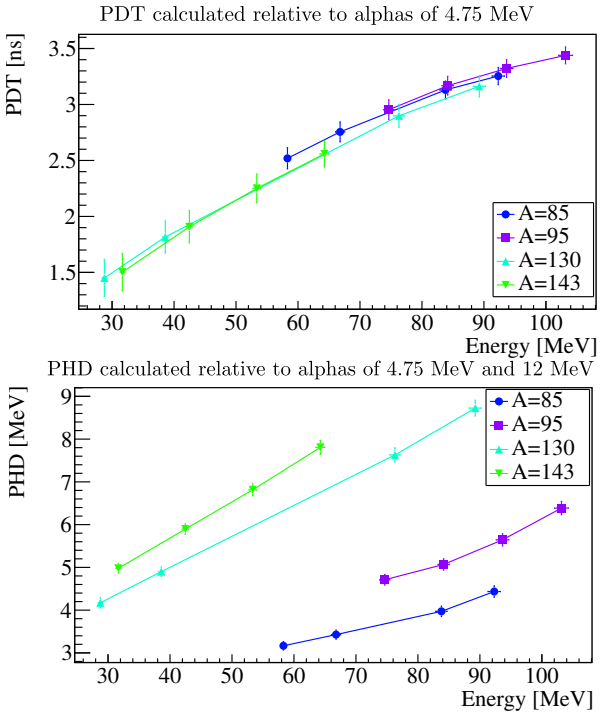


**Figure 3.** Plasma delay time (top) and Pulse height defect (bottom) as a function of the energy for different masses. The eye-guiding lines indicate a linear interpolation between the measurements. The uncertainty analysis only includes statistical errors.

### 3.4 PDT and PHD estimation

After the energy calibration is performed, the measured energies are extracted from the common Gaussian fit of the energy spectrum, using the ROOT class *TSpectrum*. The mean of each peak provided by the Gaussian fit corresponds to the measured energy of the identified FF. The measured energy difference of the ion relative to the energy provided by LOHENGRIN, corresponds to the calculated PHD.

The PDT calculation is done by applying energy cuts on the two-dimensional energy versus ToF spectrum, as can be seen in Fig. 2. After the ToF spectra are produced separately for each FF, the mean value of the Gaussian fit of each distribution corresponds to the measured ToF. In a similar manner, the PDT is calculated as the difference between the measured ToF and the calculated ToF from the known masses, energies, and the measured flight-path distance.

## 4 Preliminary results and discussion

Preliminary results of PDT and PHD are shown in Fig. 3, for masses A=85, 95, 130 and 143. Both the PDT and PHD effects exhibit strong positive correlations with the kinetic energy. The PDT increases by roughly 2 ns in the studied energy region and it seems to approach saturation at higher energies. The PHD, on the other hand, increases by more than 6 MeV across the energy range.

Similar trends of increasing PDT values as a function of ion energy were found in previous studies [8–11]. When the ion kinetic energy increases, a larger plasma cloud is expected in the detector, which will increase the disturbance of the electric field and, as a consequence, will delay the electron drift further.

The mass-dependence, however, exhibits a more complicated behaviour. The PHD is significantly mass-dependent, as it can differ by several MeV for different ion masses at similar energies. This is in agreement with the PHD values reported elsewhere [11, 12]. However, it seems to be correlated with smaller PDT variations as a function of the ion mass. Such behaviour is beneficial for the analysis of 2E-2v data from VERDI, since the iterative PDT corrections are less sensitive to the mass determination. There is a slight tendency towards a reduced PDT for heavier masses, which has also been reported earlier [8, 10]. Further analysis of the whole data set, which covers a wider range of energies and masses, is needed to fully understand the systematic PHD and PDT trends and, especially to investigate whether different PIPS units have similar detector responses.

## 5 Acknowledgments

This work was supported by the Swedish research council (Ref. No. 2019-05385). This work was also supported by the European Commission within the Seventh Framework Program through Fission-2013-CHANDA (Project No. 605203), the Swedish Radiation Safety Authority, SSM (project SSM20181587) and the Swedish Centre for Nuclear Technology (SKC). This project has received funding from the Euratom research and training programme 2014-2018 under grant agreement No 847594 (ARIEL). The authors would like to acknowledge S.J. Holm and R. Pommier for their valuable technical support.

## References

[1] M.O. Frégeau, *et. al.*, Nucl. Instr. Meth. A **817** 35 (2016).
[2] K. Jansson, *et al.*, EPJ Web Conf. **146** 04016 (2017).
[3] MIRION technologies, PIPS Detectors, https://www.mirion.com/products/pips-detectors-passivated-implanted-planar-silicon-detectors.
[4] A. Al-Adili, *et al.*, Phys. Rev. C **102** 064610 (2020).
[5] Glenn F. Knoll, *Radiation Detection and Measurement* (John Wiley & Sons, New York, 2000) pp. 385, 389, 393.
[6] K. Jansson, *et al.*, Eur. Phys. J. A **54** 114 (2018).
[7] A. Al-Adili, *et al.*, EPJ Web Conf. **169** 00002 (2018).
[8] J. Velkovska and R.L. McGrath, Nucl. Instr. Meth. A **430** 507 (1999).
[9] W. Seibt, *et al.*, Nucl. Instr. Meth. **113** 317 (1973).
[10] H.-O. Neidel, *et al.*, Nucl. Instr. Meth. **212** 299 (1983).
[11] G.N. Knyazheva, *et al.*, Nucl. Instr. Meth. B **248** 7 (2006).
[12] M. Asghar, *et al.*, Nucl. Instr. Meth. **142** 539 (1977).
[13] P. Armbruster, *et al.*, Nucl. Instr. Meth. A **139** 213 (1976).

[14] U. Köster, *et al.*, Nucl. Instr. Meth. A **613** 363 (2010).
[15] N. V. Sosnin, *et al.*, Nucl. Instr. Meth. A **957** 163397 (2020).
[16] O.V. Zeynalova, *et al.*, B. Russ. Acad. Sci. Ph. **73** 506 (2009).
[17] Z. Gao, *et al.*, Eur. Phys. J. A **58** 27 (2022).